

# First Demonstration of 6 dB Quantum Noise Reduction in a Kilometer Scale Gravitational Wave Observatory

James Lough<sup>1,\*</sup>, Emil Schreiber,<sup>1</sup> Fabio Bergamin<sup>1</sup>, Hartmut Grote,<sup>2</sup> Moritz Mehmet<sup>1</sup>, Henning Vahlbruch<sup>1</sup>, Christoph Affeldt,<sup>1</sup> Marc Brinkmann,<sup>1</sup> Aparna Bisht,<sup>1</sup> Volker Kringel,<sup>1</sup> Harald Lück<sup>1</sup>, Nikhil Mukund<sup>1</sup>, Severin Nadji<sup>1</sup>, Borja Sorazu,<sup>3</sup> Kenneth Strain<sup>3</sup>, Michael Weinert,<sup>1</sup> and Karsten Danzmann<sup>1</sup>

<sup>1</sup>*Institut für Gravitationsphysik, Leibniz Universität Hannover and Max-Planck-Institut für Gravitationsphysik (Albert-Einstein-Institut), Callinstraße 38, 30167 Hannover, Germany*

<sup>2</sup>*School of Physics and Astronomy, Cardiff University, The Parade, CF24 3AA, United Kingdom*

<sup>3</sup>*SUPA, University of Glasgow, Glasgow G12 8QQ, United Kingdom*



(Received 22 June 2020; accepted 4 January 2021; published 26 January 2021)

Photon shot noise, arising from the quantum-mechanical nature of the light, currently limits the sensitivity of all the gravitational wave observatories at frequencies above one kilohertz. We report a successful application of squeezed vacuum states of light at the GEO 600 observatory and demonstrate for the first time a reduction of quantum noise up to  $6.03 \pm 0.02$  dB in a kilometer scale interferometer. This is equivalent at high frequencies to increasing the laser power circulating in the interferometer by a factor of 4. Achieving this milestone, a key goal for the upgrades of the advanced detectors required a better understanding of the noise sources and losses and implementation of robust control schemes to mitigate their contributions. In particular, we address the optical losses from beam propagation, phase noise from the squeezing ellipse, and backscattered light from the squeezed light source. The expertise gained from this work carried out at GEO 600 provides insight toward the implementation of 10 dB of squeezing envisioned for third-generation gravitational wave detectors.

DOI: [10.1103/PhysRevLett.126.041102](https://doi.org/10.1103/PhysRevLett.126.041102)

*Introduction.*—Gravitational waves, ripples in the fabric of spacetime, were long theorized, and it took 100 years to measure them directly [1]. The currently favored devices for measuring the spacetime metric perturbations are kilometer scale variants of the Michelson interferometer. These interferometers sense the differential arm length modulation due to audioband gravitational waves.

The main source of noise in all interferometric gravitational wave detectors at high frequency is the so-called shot noise, which can be interpreted as random detection of photons. The quantum nature of coherent light results in uncertainty in amplitude and phase which are canonically conjugate observables. These can be transformed into the sine and cosine quadrature amplitude basis. From normalized quadrature operators,  $X_1$  and  $X_2$ , we have the uncertainty relation

$$\Delta X_1 \Delta X_2 \geq 1. \quad (1)$$

The coherent state is a state with minimum uncertainty equal in the two quadratures. Reducing the uncertainty in one quadrature below this state of minimum uncertainty is known as squeezing. Because of Heisenberg's uncertainty principle [Eq. (1)], this implies that the uncertainty in the orthogonal quadrature must be increased, an effect known as antisqueezing.

Quantum noise in a gravitational wave detector can be thought of as arising from vacuum fluctuations of light incident on the so-called dark port of the interferometer. This is the output port where traditionally no light is injected and thus it is only this vacuum field that enters the output of the detector (see Fig. 1). With this picture, the application of a squeezed vacuum field was first proposed in 1981 [2]. Since then, GEO 600 was the first kilometer scale detector to apply squeezing in 2010 [3] followed by a proof of principle at the initial LIGO detector in Hanford, WA [4]. Long term stable application of squeezing was pioneered at GEO 600 [5] and continuously improved as reported here. Recently, the LIGO and Virgo detectors have reached 3 dB noise reduction from the application of squeezing [6,7]. The application of squeezed light is a key technology in the design of all third generation detectors demanding a quantum shot noise reduction of 10 dB [8].

At GEO 600, the fully operational gravitational wave detector serves as a test bed for instrument science research

*Published by the American Physical Society under the terms of the Creative Commons Attribution 4.0 International license. Further distribution of this work must maintain attribution to the author(s) and the published article's title, journal citation, and DOI. Open access publication funded by the Max Planck Society.*

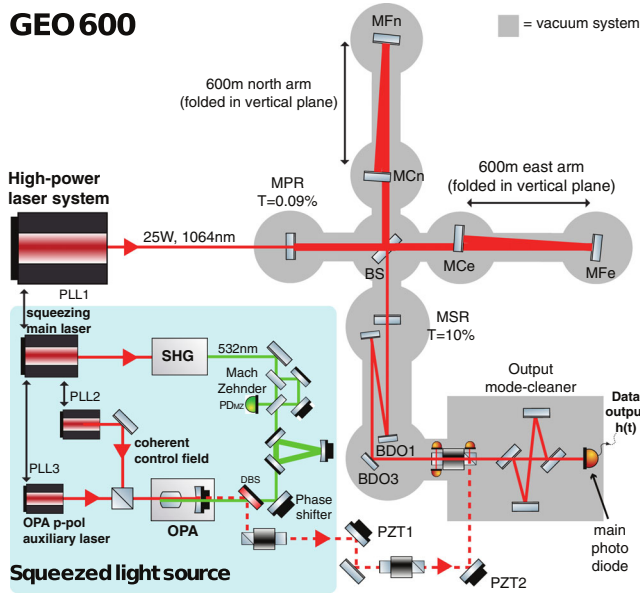


FIG. 1. The layout of the squeezing application to the GEO 600 detector. The three Faraday isolators used for squeezed light injection are depicted. The squeezed light is injected such that it overlaps the main beam with the correct polarization at the MSR. The photodiodes shown at the in-vacuum Faraday isolator are used for polarization diagnostics.

and development. In particular, we are interested in the research and development of the application of squeezing as a technology for improving sensitivity at high frequency. Important sources of gravitational waves at high frequency include most notably the postmerger signal around a few kHz from binary neutron star inspirals which will be signatures rich in information about the structure of neutron stars [9,10]. Additionally, at lower frequencies around 1 kHz, tidal deformation effects at the later part of the inspiral phase that also depend on the neutron star equation of state will be visible [11,12].

Additional signals of interest relevant for GEO could come from low mass dark matter fields. It has been proposed that large interferometers could be sensitive to time varying signatures of such fields [13]. The coupling comes through influence on physical constants such as the fine structure constant, which affect properties of the beam splitter bulk material. Because of the topology of GEO 600 (see Fig. 1), the detector is highly sensitive to the beam splitter as it is located in the most sensitive part of the interferometer [14].

For the application of squeezed light, our goal is to reduce the uncertainty of the amplitude of light at the main read-out photodetector. Because this amplitude corresponds to the differential phase of light in the arms of the gravitational wave detector, we call this phase squeezing. At low frequencies inside the interferometer, due to the finite mass of our suspended mirrors, there is a coupling between the amplitude and phase quadratures. At GEO

600, the noise from this effect is masked by technical noise; therefore, we can apply frequency-independent squeezing, phase squeezing at all frequencies, without impacting the sensitivity at low frequencies. This is, however, an important topic of research as the larger detectors are able to observe this noise [15,16] and will be further limited by this in the future with improvements to technical noise, circulating power, and applied squeezing. Techniques for compensating this effect have made significant progress in development including planned upgrades [17,18] and more recently proposed ideas [19].

In this Letter, we present the observation of up to  $6.03 \pm 0.02$  dB of noise reduction at 6 kHz due to the application of squeezing, demonstrated for the first time on a full scale gravitational wave detector. This advancement in quantum noise reduction equivalent to a factor of 4 increase in laser power marks a major milestone in the progress of squeezed light application.

*Experimental setup.*—The GEO 600 detector is a Michelson interferometer with power recycling and signal recycling [20]. A simplified optical layout of the detector is provided in Fig. 1. The two arms have a folding mirror, resulting in a total length of 1200 m per arm. These, along with the beam splitter (BS) mirror, comprise the Michelson portion of the interferometer. The power recycling cavity (PRC) and signal recycling cavity (SRC) are formed by the power recycling mirror (MPR) and signal recycling mirror (MSR), respectively, with the Michelson. The PRC increases the circulating power in the interferometer by a factor of about 1000 which leads to increased sensitivity. We typically run the detector with about 3 W of input power resulting in a circulating power of roughly 3 kW. The application of signal recycling resonantly enhances the signal by forming a 1200 m cavity with a finesse of 56. This resonant enhancement also limits the bandwidth of the detector, acting as a low pass filter, which causes the white shot noise to increase toward higher frequency in the calibrated strain data (see Fig. 2). The signal due to differential arm length changes is imprinted onto the carrier light transmitted by the signal-recycling mirror. This field is directed to the output mode cleaner cavity (OMC) by the beam directing optics which are also used to reduce the beam size from 1 cm. The OMC filters the output field to suppress transverse and longitudinal modes of light that are not the gravitational wave carrying mode. Finally, the detector strain data are derived from the field impinging on the photodiode (PD) by means of a dc readout scheme [21,22].

The squeezed light source is located on an external optical bench operated in-air [23–25]. The squeezed vacuum states of light are generated by parametric down-conversion [26] inside an optical parametric amplifier (OPA) cavity, using a periodically poled potassium titanyl phosphate crystal as the nonlinear medium. The required OPA pump field at 532 nm is generated in a

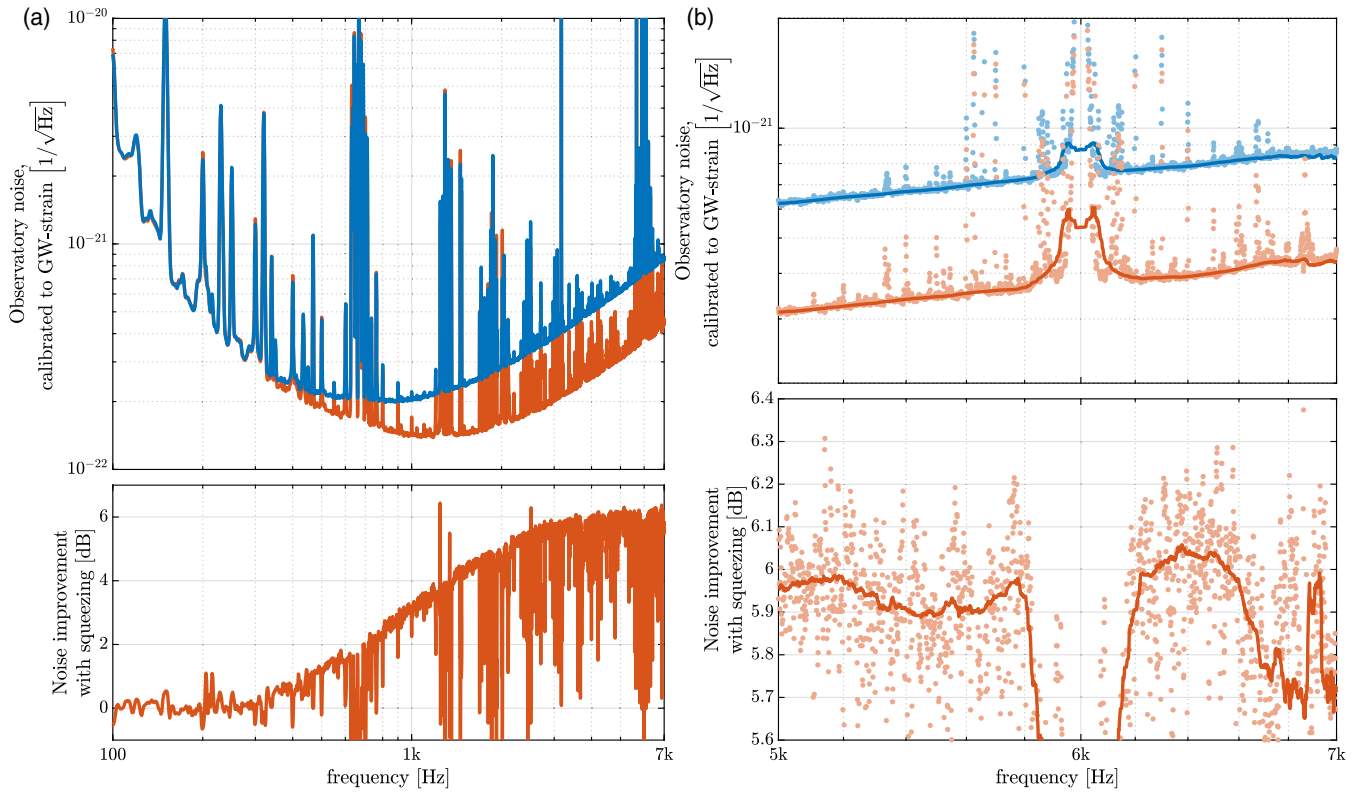


FIG. 2. With the application of squeezing, we observe a factor of 2 improvement in sensitivity at high frequencies. (a) The top plot compares 15 minute power spectral density (PSD) estimates of the detector noise with (red) and without (blue) squeezing. Towards higher frequencies, the increase in shot noise proportional to  $f$  is due to calibration compensation of the filtering effect of the SRC. The bottom plot shows the squeezing ratio as a function of frequency. The squeezing value of  $6.03 \pm 0.02$  dB is calculated from the ratio between median noise floor estimates with and without squeezing averaged between 6.3 and 6.5 kHz and referenced against periods where the squeezing was not applied during valid science time over a two month duration. Toward lower frequencies, the squeezing is increasingly limited by technical noise. Plot (b) shows a zoomed-in section of the same data (dots). Noise floor estimates in the top plot and their ratio in the bottom plot are depicted as solid lines.

second-harmonic generator. The power of the pump field injected into the OPA can be adjusted via a Mach-Zehnder interferometer to realize different squeezing levels. The squeezed field is circulated into the GEO 600 dark port via the polarizing beam splitter (PBS) of a low-loss, in-vacuum Faraday isolator. Two additional in-air Faraday isolators are used to further decouple the OPA from residual interferometer light. Two piezo-actuated steering mirrors (PZT1, PZT2 in Fig. 1) are used for automatic alignment of the squeezed field to the interferometer [27].

Our current work focuses on the interfacing of the squeezed light source to the detector, in particular matching the optical mode of the squeezed light source efficiently to that of the gravitational wave signal mode of the interferometer. Upgrades important to improvements in the squeezing level include in-vacuum diagnostic photodiodes for *in situ* monitoring of polarization matching, additional wave plates to correct for birefringence effects, and compensation of astigmatic effects in the output optics of the detector.

In the rejection ports of the in-vacuum faraday isolator (see Fig. 1), we placed photodiodes to monitor the rejected

power for understanding the polarization state of the squeezed field in the in-vacuum path [28]. We also used the signals from these PDs to optimize the PBS cube angles of incidence.

The addition of a quantum noise lock [29], which actuates on the demodulation phase for the squeezer, improved the stability of the squeezed light source early on [30]. We now use the same technique to control for drifts in the temperature of the OPA, further improving the stability of the squeezing level by maintaining the coresonance condition in the OPA. A consistently optimized squeezed light source is important for allowing us to use the squeezing level as a metric for tuning the many degrees of freedom in the squeezing interface which impact squeezing.

To maintain consistent, very high squeezing levels, the stability of the squeezed light source in reference to the detector and its environment as well as the interface to the detector are important. The combination of efforts discussed in this section have improved the squeezing level from 3.4 dB [31] to the current record of 6.0 dB which will be discussed in more detail in Sec. IV.

*Analysis.*—The observed squeezing level will always be less than that of the generated squeezed vacuum due to residual optical loss, phase noise, and technical noise. Squeezed light sources of the type employed at GEO have demonstrated very high levels of squeezing mainly limited by detection [32]. In GEO 600, the squeezing level is mainly limited at high frequency by optical loss and therefore this has been our primary focus of work for achieving a high squeezing level. In the following, we discuss the loss mechanisms that affect the observable squeezing.

Optical loss: Optical loss provides a path for unsqueezed vacuum to couple to the optical mode of the detector and therefore reduces the effective quantum reduction that can be achieved. This degradation increases as the squeezing level improves. Considering a squeezed vacuum variance  $V_s$  that includes losses, a small additional optical loss  $l$  mixes in some of the vacuum variance,  $V_0 > V_s$ , resulting in an increased variance [33],

$$V = (1 - l)V_s + lV_0. \quad (2)$$

The squeezing ratio is thus reduced by the factor

$$\sqrt{\frac{V_s}{V}} = \left(1 + l \frac{V_0 - V_s}{V_s}\right)^{-1/2}, \quad (3)$$

which for small loss is approximated as

$$\sqrt{\frac{V_s}{V}} \approx 1 - \frac{V_0 - V_s}{2V_s} l. \quad (4)$$

Thus, the stronger the squeezing, the more the loss term matters. At the 6 dB level of observed squeezing, a removal of an element with optical loss of 1% results in an increase of detection volume of about 7%.

Direct measurements of optical loss for most of the squeezed light injection path can be performed while the interferometer is not resonating and are listed in Table I. For this measurement, a bright field that is resonant in the OPA is injected toward the interferometer. When the interferometer is unlocked and the end mirrors are misaligned, the reflection from the signal recycling mirror is 90%. Reflection from the locked cavity would ideally be 100%, but depends on internal losses of the signal recycling cavity as well as coupling efficiencies between the relevant cavities which can be frequency dependent. Our estimate of this effective loss from the SRC is listed in Table I as SRC loss for the measured squeezing frequency of 5.2 kHz.

Mode matching and alignment of the interferometer to the output mode cleaner is accomplished in reference to the so-called beacon mode of the interferometer which is generated by modulating the differential arm length at 3.17 kHz and marks the mode which carries the

TABLE I. Optical loss contributions. These are the known contributors of optical loss taking into account double passes as appropriate. Included is the equivalent loss due to dark noise from the main photodiode [34] which is white at high frequency and mimics optical loss. The total loss from this estimate is less than the total loss inferred from the observed squeezing level of about 22% (see Fig. 3).

| Source                          | Loss (%) |
|---------------------------------|----------|
| OPA escape efficiency           | 1.0      |
| Squeezed light source after OPA | 1.3      |
| In-air injection path           | 1.8      |
| In-vacuum optics up to OMC      | 6.6      |
| BDO1 transmission               | 2.0      |
| SRC loss                        | 1.4      |
| OMC internal loss               | 1.9      |
| OMC mode matching—second order  | 1.3      |
| OMC additional mismatch         | 5.0      |
| OMC alignment control dither    | 0.3      |
| PD quantum efficiency           | 1.0      |
| Dark noise equivalent           | 0.1      |
| Total                           | 21.4     |

gravitational wave signal. We measure the beacon modulation at the main photodiode and correct with the dc level to derive a new signal representing the light power of the beacon mode [35]. The squeezed field is aligned to the interferometer sidebands using an autoalignment system which aligns the coherent control sidebands, which are copropagating with the squeezed vacuum field, to the modulation sidebands from the interferometer [27]. Residual misalignment fluctuations will also cause optical loss. These contributions to optical loss are not expected to be very significant and are not well characterized and so are not listed in Table I.

In order to match the mode of the squeezed vacuum field to that of the OMC, the same configuration as for optical loss measurements is used. We achieve a matching of at least 93.8%, which is determined by measuring the bright alignment light in reflection of the OMC. Only 1.3% of the mismatch is due to waist size and location, which is primarily limited by residual astigmatism. The source of the additional 5% mismatch is unknown.

Phase noise: The squeezing ellipse angle is selected for maximum reduction of quantum shot noise in the readout channel. Static offset and time-dependent fluctuations—jitter—in this angle reduce the effective squeezing by coupling antisqueezing to the readout quadrature. The phase angle is locked using the beat of the coherent control sidebands from the OPA with the carrier field of the interferometer at the main photodiode. Sources of phase jitter have been published in [30], with more recent results in [28] and add up to 17 mrad. Additionally, one can measure the impact of increased squeezing on the shot noise and use a model of the phase noise effect to estimate the phase noise. One limitation we have found with this

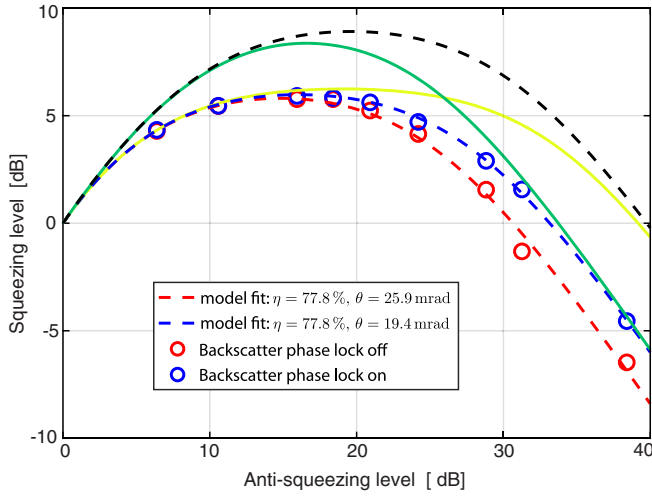


FIG. 3. Detected squeezing level as a function of measured antisqueezing measured at 5.2 kHz. The blue and red traces represent fits to the respective data points. The fitting procedure fits a common parameter for optical efficiency,  $\eta$ . The two solid traces represent estimates of the detectable squeezing level if a factor of 2 reduction of optical loss (green) and phase noise (yellow) could be realized. The dashed black trace is a factor of 2 improvement in both. This shows that we are still primarily limited by optical loss.

method is that any additional noise that is dependent on the nonlinear gain will add to the effect and give an overestimate of the phase noise. An example of such nonlinear gain-dependent noise is explained under technical noise. The estimate of phase noise from the model fitting technique is shown in Fig. 3.

**Nonquantum noise:** Observable squeezing is limited by technical and other nonquantum noise sources which can be broadband or frequency dependent. Fundamental thermal noise at GEO 600 decreases as  $f^{-1/2}$  toward higher frequency, making it an important noise source at intermediate frequencies [36]. Technical noise in GEO generally increases toward lower frequencies and diminishes the noise improvement due to squeezing as shown in Fig. 2. At high frequency, the observed squeezing level is affected by two technical noises in particular that are white at the shot noise dominated frequencies in reference to the main photodiode. These are the photodetector dark noise and a new source of technical noise we have identified as a form of backscatter noise which behaves similar to the phase noise.

The backscatter noise comes from stray interferometer light leaking along the squeezing injection path to the OPA where it is reflected with a gain factor that depends on the phase of the backscattered light. This reflection can cause linear and nonlinear coupling of the stray light field's random phase fluctuations  $\Phi + \delta\phi$  to the detector signal, as well as a linear coupling of the residual squeezing-angle fluctuations  $\delta\theta$ . The backscatter noise signal is

$$i_{\text{bs}}(t) \approx \sqrt{\frac{(1-L)P_{\text{stray}}}{P_{\text{out}}}} \times [e^{-r} \cos(\Phi) - e^{-r} \sin(\Phi)\delta\phi - 2\sinh(r)\sin(\Phi)\delta\theta], \quad (5)$$

with squeezing parameter  $r$  and total optical loss for the squeezed field  $L$  [28]. The final term provides the amplification with increased squeezing. The phase noise of the squeezed light field is modulated with the absolute phase  $\Phi$  of the backscattered light. Using this effect, we derive an error signal of the phase of the backscattered light by measuring the response due to a dithering of the squeezing phase. From this signal, we actuate on the path length from the squeezed light source to the interferometer with a mirror mounted to a piezoelectric transducer (PZT).

**Results.**—In Fig. 2, we report up to  $6.03 \pm 0.02$  dB sensitivity enhancement observed at GEO 600 due to the application of squeezing. We estimate the optical loss and phase noise by measuring the squeezing and antisqueezing at different nonlinear gains in Fig. 3.

Our best estimate of the sources of phase noise add up to 17 mrad. With the influence of backscatter noise described in Sec. III, we observe a nonlinear gain-dependent noise equivalent to 25.9 mrad of phase noise. After controlling the phase of the backscattered light field, we achieve a better phase noise estimate of 19.4 mrad. In Fig. 3, we show the results of fitting our measurements to our model. With the backscatter phase loop engaged, there is a clear reduction in the estimated phase noise when fitting squeezing versus antisqueezing.

**Conclusions and Outlook.**—The observation of 6 dB quantum shot noise reduction from the application of squeezed states of light at the GEO 600 detector is a first for a kilometer scale gravitational wave detector. This demonstrates the ability to achieve a key goal for the next phase of upgrades to the advanced detectors known as aLIGO+ and AdV+ [8]. The application of frequency-independent squeezing leads to an improvement in sensitivity, which can be used in addition to an increase in laser power.

This is relevant to other gravitational wave detectors given the similar complexity. The LIGO and Virgo detectors are well on their way at 3.2 dB [6,7] and will face similar challenges of optical loss and mode matching in order to achieve the 6 dB mark. The next milestone in squeezing level to look toward is 10 dB. This is the level of squeezing assumed for third generation detectors [37] such as the Einstein Telescope [38] and Cosmic Explorer [39].

Optical efficiency requirements for achieving 10 dB squeezing are better than 90%, dependent on the phase noise. For GEO 600, we are limited primarily by optical loss, so we continue to focus in that direction toward the next goal of observing 10 dB squeezing. We have a few unknown losses as indicated in Table I as well as the

discrepancy between the measured optical loss and the observed effective optical loss that may be related to residual alignment fluctuation unaccounted for.

We are currently designing improvements to the optical system at the output of the detector, including a new OMC design. Significant improvements in the output optics to reduce wavefront distortions and improve alignment control along with improvements to the optical efficiency of individual elements should allow for 10 dB squeezing to be observed at the GEO detector even with the current squeezed light source.

The authors would like to thank Walter Grass for his years of expert support in the maintenance of critical infrastructure to the site to include the extensive 400 m<sup>3</sup> vacuum system. The authors are grateful for support from the Science and Technology Facilities Council Grant Ref: ST/L000946/1, the University of Glasgow in the United Kingdom, the Bundesministerium für Bildung und Forschung, the state of Lower Saxony in Germany, the Max Planck Society, Leibniz Universität Hannover, and Deutsche Forschungsgemeinschaft (DFG, German Research Foundation) under Germany's Excellence Strategy—EXC 2123 QuantumFrontiers—390837967. This work was partly supported by DFG grant SFB/Transregio 7 Gravitational Wave Astronomy. This document has been assigned LIGO document number LIGO-P2000032.

\*james.lough@aei.mpg.de

- [1] B. P. Abbott *et al.* (LIGO Scientific and Virgo Collaborations), Observation of Gravitational Waves from a Binary Black Hole Merger, *Phys. Rev. Lett.* **116**, 061102 (2016).
- [2] C. M. Caves, Quantum-mechanical noise in an interferometer, *Phys. Rev. D* **23**, 1693 (1981).
- [3] J. Abadie *et al.* (LIGO Scientific Collaboration), A gravitational wave observatory operating beyond the quantum shot-noise limit, *Nat. Phys.* **7**, 962 (2011).
- [4] J. Aasi *et al.*, Enhanced sensitivity of the LIGO gravitational wave detector by using squeezed states of light, *Nat. Photonics* **7**, 613 (2013).
- [5] H. Grote, K. Danzmann, K. L. Dooley, R. Schnabel, J. Slutsky, and H. Vahlbruch, First Long-Term Application of Squeezed States of Light in a Gravitational-Wave Observatory, *Phys. Rev. Lett.* **110**, 181101 (2013).
- [6] M. Tse *et al.*, Quantum-Enhanced Advanced LIGO Detectors in the Era of Gravitational-Wave Astronomy, *Phys. Rev. Lett.* **123**, 231107 (2019).
- [7] F. Acernese *et al.*, Increasing the Astrophysical Reach of the Advanced Virgo Detector via the Application of Squeezed Vacuum States of Light, *Phys. Rev. Lett.* **123**, 231108 (2019).
- [8] LIGO Scientific Collaboration, Instrument Science White Paper 2018, Technical Report No. T1800133-v4, 2018, <https://dcc.ligo.org/LIGO-T1800133/public>.
- [9] J. A. Clark, A. Bauswein, N. Stergioulas, and D. Shoemaker, Observing gravitational waves from the post-merger phase of binary neutron star coalescence, *Classical Quantum Gravity* **33**, 085003 (2016).
- [10] B. Abbott *et al.*, Properties of the Binary Neutron Star Merger GW170817, *Phys. Rev. X* **9**, 011001 (2019).
- [11] J. S. Read, C. Markakis, M. Shibata, K. Uryū, J. D. E. Creighton, and J. L. Friedman, Measuring the neutron star equation of state with gravitational wave observations, *Phys. Rev. D* **79**, 124033 (2009).
- [12] K. Chatziioannou, C.-J. Haster, and A. Zimmerman, Measuring the neutron star tidal deformability with equation-of-state-independent relations and gravitational waves, *Phys. Rev. D* **97**, 104036 (2018).
- [13] Y. V. Stadnik and V. V. Flambaum, Searching for Dark Matter and Variation of Fundamental Constants with Laser and Maser Interferometry, *Phys. Rev. Lett.* **114**, 161301 (2015).
- [14] H. Grote and Y. V. Stadnik, Novel signatures of dark matter in laser-interferometric gravitational-wave detectors, *Phys. Rev. Research* **1**, 033187 (2019).
- [15] F. Acernese *et al.*, Quantum Backaction on Kg-Scale Mirrors: Observation of Radiation Pressure Noise in the Advanced Virgo Detector, *Phys. Rev. Lett.* **125**, 131101 (2020).
- [16] H. Yu *et al.*, Quantum correlations between light and the kilogram-mass mirrors of LIGO, *Nature (London)* **583**, 43 (2020).
- [17] Y. Zhao *et al.*, Frequency-Dependent Squeezed Vacuum Source for Broadband Quantum Noise Reduction in Advanced Gravitational-Wave Detectors, *Phys. Rev. Lett.* **124**, 171101 (2020).
- [18] L. McCuller, C. Whittle, D. Ganapathy, K. Komori, M. Tse, A. Fernandez-Galiana, L. Barsotti, P. Fritschel, M. MacInnis, F. Matichard, K. Mason, N. Mavalvala, R. Mittleman, H. Yu, M. Zucker, and M. Evans, Frequency-Dependent Squeezing for Advanced LIGO, *Phys. Rev. Lett.* **124**, 171102 (2020).
- [19] J. Südbeck, S. Steinlechner, M. Korobko, and R. Schnabel, Demonstration of interferometer enhancement through Einstein–Podolsky–Rosen entanglement, *Nat. Photonics* **14**, 240 (2020).
- [20] B. J. Meers, Recycling in laser-interferometric gravitational-wave detectors, *Phys. Rev. D* **38**, 2317 (1988).
- [21] J. Degallaix, H. Grote, M. Prijatelj, M. Hewitson, S. Hild, C. Affeldt, A. Freise, J. Leong, H. Lück, K. A. Strain, H. Wittel, B. Willke, and K. Danzmann, Commissioning of the tuned DC readout at GEO 600, *J. Phys. Conf. Ser.* **228**, 012013 (2010).
- [22] S. Hild, H. Grote, J. Degallaix, S. Chelkowski, K. Danzmann, A. Freise, M. Hewitson, J. Hough, H. Lück, M. Prijatelj, K. A. Strain, J. R. Smith, and B. Willke, DC-readout of a signal-recycled gravitational wave detector, *Classical Quantum Gravity* **26**, 055012 (2009).
- [23] H. Vahlbruch, S. Chelkowski, B. Hage, A. Franzen, K. Danzmann, and R. Schnabel, Coherent Control of Vacuum Squeezing in the Gravitational-Wave Detection Band, *Phys. Rev. Lett.* **97**, 011101 (2006).
- [24] H. Vahlbruch, A. Khalaidovski, N. Lastzka, C. Gräf, K. Danzmann, and R. Schnabel, The GEO 600 squeezed light source, *Classical Quantum Gravity* **27**, 084027 (2010).

- [25] A. Khalaidovski, H. Vahlbruch, N. Lastzka, C. Gräf, H. Lück, K. Danzmann, H. Grote, and R. Schnabel, Status of the GEO 600 squeezed-light laser, *J. Phys. Conf. Ser.* **363**, 012013 (2012).
- [26] L.-A. Wu, H. J. Kimble, J. L. Hall, and H. Wu, Generation of Squeezed States by Parametric Down Conversion, *Phys. Rev. Lett.* **57**, 2520 (1986).
- [27] E. Schreiber, K. L. Dooley, H. Vahlbruch, C. Affeldt, A. Bisht, J. R. Leong, J. Lough, M. Prijatelj, J. Slutsky, M. Was, H. Wittel, K. Danzmann, and H. Grote, Alignment sensing and control for squeezed vacuum states of light, *Opt. Express* **24**, 146 (2016).
- [28] E. Schreiber, Gravitational-wave detection beyond the quantum shot-noise limit—The integration of squeezed light in GEO 600, Ph.D. thesis, Leibniz Universität Hannover, 2018.
- [29] K. McKenzie, E. E. Mikhailov, K. Goda, P. K. Lam, N. Grosse, M. B. Gray, N. Mavalvala, and D. E. McClelland, Quantum noise locking, *J. Opt. B* **7**, S421 (2005).
- [30] K. L. Dooley, E. Schreiber, H. Vahlbruch, C. Affeldt, J. R. Leong, H. Wittel, and H. Grote, Phase control of squeezed vacuum states of light in gravitational wave detectors, *Opt. Express* **23**, 8235 (2015).
- [31] K. L. Dooley *et al.*, GEO 600 and the GEO-HF upgrade program: Successes and challenges, *Classical Quantum Gravity* **33**, 075009 (2016).
- [32] M. Mehmet and H. Vahlbruch, High-efficiency squeezed light generation for gravitational wave detectors, *Classical Quantum Gravity* **36**, 015014 (2019).
- [33] E. S. Polzik, J. Carri, and H. J. Kimble, Atomic spectroscopy with squeezed light for sensitivity beyond the vacuum-state limit, *Appl. Phys. B* **55**, 279 (1992).
- [34] H. Grote, M. Weinert, R. X. Adhikari, C. Affeldt, V. Kringel, J. Leong, J. Lough, H. Lück, E. Schreiber, K. A. Strain, H. Vahlbruch, and H. Wittel, High power and ultra-low-noise photodetector for squeezed-light enhanced gravitational wave detectors, *Opt. Express* **24**, 20107 (2016).
- [35] N. Smith-Lefebvre, S. Ballmer, M. Evans, S. Waldman, K. Kawabe, V. Frolov, and N. Mavalvala, Optimal alignment sensing of a readout mode cleaner cavity, *Opt. Lett.* **36**, 4365 (2011).
- [36] D. Heinert, K. Craig, H. Grote, S. Hild, H. Lück, R. Nawrodt, D. A. Simakov, D. V. Vasilyev, S. P. Vyatchanin, and H. Wittel, Thermal noise of folding mirrors, *Phys. Rev. D* **90**, 042001 (2014).
- [37] M. Punturo *et al.*, The third generation of gravitational wave observatories and their science reach, *Classical Quantum Gravity* **27**, 084007 (2010).
- [38] M. R. Abernathy *et al.*, Einstein gravitational wave telescope conceptual design study (2011).
- [39] D. Reitze *et al.*, Cosmic explorer: The U.S. contribution to gravitational-wave astronomy beyond LIGO, *Bull. Am. Astron. Soc.* **51** (2019), <https://baas.aas.org/pub/2020n7i035>.